Coupled Mesh Lagrangian/ALE Modeling: Opportunities and Challenges

A. C. Robinson,[*] J. E. Bishop*, D. M. Hensinger,[*] T. E. Voth[*] M. K. Wong[*]

[*]Sandia National Laboratories, New Mexico, 87185

We describe two methods for coupled mesh Lagrangian/ALE modeling where one mesh is treated as a Lagrangian mesh while the other is ALE. Lagrangian contact modeling is implemented in the first method to couple the two meshes. In the second method an overlapping grid algorithm that requires mapping of the information from one grid to another has been implemented. We review current experience with these two technologies.

Introduction

Lagrangian modeling is often preferred whenever the kinematics of the continuum flow permit because of its ability to precisely model discrete features which may be diffused when an Eulerian approach is used. Hence, in the context of multi-material modeling, it is desirable to preserve as much of the Lagrangian approach as possible.. We review current experience with two coupled mesh technologies where the modeling on one of these meshes is treated as pure Lagrangian and the modeling on the other mesh is an Arbitrary Lagrangian/Eulerian (ALE) treatment.

An interface-coupled methodology is considered first. This technique, referred to here as SHISM, is applicable to problems involving contact between materials of dissimilar compliance (Bishop et al., 2005). The technique models the more compliant (soft) material as ALE while the less compliant (hard) material and associated interface are modeled in a Lagrangian fashion. Loads are transferred between the hard and soft materials via explicit transient dynamics contact algorithms (Brown et al., 2003). The use of these contact algorithms does not require a node-to-node matching at the Lagrangian interface. In the context of the operator-split ALE algorithm, a single Lagrangian step is performed using a mesh to mesh contact algorithm. At the end of the Lagrangian step the meshes will be slightly offset at the interface but non-interpenetrating. The nodes at the interface on the ALE mesh are then moved to their initial location relative to the Lagrangian body faces and the ALE mesh is smoothed, translated and rotated to follow the Lagrangian body. Robust remeshing in the ALE region is required for success of this algorithm, and we describe current work in this area.

The second coupling method described here is an overlapping grid methodology that requires mapping of information between a Lagrangian mesh and an ALE mesh. The Lagrangian mesh describes a relatively hard body that interacts with a softer material contained in the ALE mesh. A predicted solution for the velocity field is performed

independently on both meshes. Element-centered velocity and momentum are transferred between the meshes using a volume transfer capability (Brown et al., 2003). Data from the ALE mesh is mapped to a *phantom* mesh that surrounds the Lagrangian mesh, providing for the reaction to the predicted motion of the Lagrangian material. Data from the Lagrangian mesh is mapped directly to the ALE mesh. A momentum balance is performed on both meshes to adjust the velocity field to account for the interaction of the material from the other mesh. Subsequently, remeshing and remapping of the ALE mesh is performed to allow large deformation of the softer material. We review current progress using this approach and discuss avenues for future research and development.

ALEGRA

ALEGRA is the generic name for a suite of capabilities based on an operator-split ALE approach to continuum modeling (Benson, 1989). ALEGRA is built on the NEVADA code base; a set of physics-independent software upon which multiple applications can be constructed. The NEVADA infrastructure also supports extensive software mechanisms for source code control of third party libraries as well as NEVADA and application source code in an integrated test-based code development environment.

ALEGRA provides a multiple-material ALE capability that is implemented in parallel on quadrilateral and hexahedral meshes (Carroll et al. 2005). The basic Lagrangian methodology and terminology is based on the PRONTO3D Lagrangian code (Taylor and Flanagan, 1987). The approach to remesh and remap has been described in (Peery and Carroll, 2000). The general algorithm flow is:

(1) Setup the initial conditions of the problem including the mesh, material distribution and state and nodal velocities.

(2) Compute the external and internal forces at time level n, $\mathbf{F}_{ext}^{n}$ and $\mathbf{F}_{\text{int}}^{n}$ with an approximate contact forces, $\mathbf{F}_{c}^{n}$.

(3) Compute the nodal accelerations using the equation

$$\mathbf{M}\mathbf{a}^{n} = \mathbf{F}_{ext}^{n} - \mathbf{F}_{\text{int}}^{n} + \mathbf{F}_{c}^{n}$$

(4) Integrate acceleration using a centered differencing to compute the velocity at the half time step, $\mathbf{v}^{n+1/2}$, and the nodal positions, $\mathbf{x}^{n+1}$, at time, t^{n+1}.

(5) Update $\mathbf{F}_{c}^{n}$ to satisfy the contact constraints.

(6) Update 3 and 4 to obtain the correct accelerations, velocities and nodal positions

(7) Integrate the rotation and stretch tensors using the rate of strain tensor.

(8) Update the material state for both equation of state models and hypoelastic relationships.

(9) Determine whether a given mesh section is to be remeshed and apply an algorithm to produce a new mesh. This could be the original mesh, the final mesh, or a mesh obtained by, for example, a smoothing algorithm.

(10) Remap all dependent quantities onto the new mesh via an appropriate algorithm for element centered or node centered quantities.

The approach to parallelism is domain decomposition using a mesh partitioner combined with MPI message passing between processes on distributed compute nodes. Internally the code infrastructure supports one layer of "ghost cells" for use in communication and algorithm implementation. The capability described above is supported on an

unstructured mesh in which the data is laid out by topological entity. For example, all unstructured mesh data at a given node is laid out sequentially in memory. The same holds true for element centers, edges and faces. The code is also a multi-material code in the sense that each element is able to support data associated with multiple materials. Key in this regard is the volume fraction of each material in each cell. The sum of these material volume fractions plus the void volume fraction must always equal one.

This topological entity based data structure layout is very convenient relative to supporting adaptive element modeling for general NEVADA applications. However, it has disadvantages in terms of performance characteristics. In order to improve performance relative to the object based memory layout, the ALEGRA algorithms have been implemented on a NEVADA curvilinear multi-block structured mesh. In this case, the memory for node, edge and face quantities is laid out contiguously across mesh blocks. Element centered quantities are laid out either element by element which is useful for material data or contiguously by block.

The curvilinear multi-block structured capability of ALEGRA requires that each block of mesh have a structured block topology, but it allows arbitrary connections between these blocks. This provides significant flexibility in the representation of computational domains. During the Lagrangian portion of ALEGRA's time step, the structured code relies on swap/add operations for communication between on processor and off processor blocks. Because of the implicit element topology within each structured block, the per-element memory requirements of curvilinear multi-block ALEGRA are significantly less than those of unstructured ALEGRA. The low memory overhead, and increased execution speed of curvilinear multi-block ALEGRA make it attractive for use as the ALE mesh in problems coupling Lagrangian to ALE domains.

ALEGRA/SHISM

The ALEGRA/SHISM algorithm employs two meshes that are joined at a Lagrangian interface via a contact search/enforcement algorithm. The less compliant of the materials is meshed in an ALE fashion while the harder material is taken to be Lagrangian. The essence of the SHISM algorithm is what happens in the ALE remesh step (step 9 above);

9a) Only the external mesh is remeshed

9b) Determine an average translation and rotation for the Lagrangian body.

9c) Move the interface ALE nodes back to their original position on the Lagrangian mesh surface.

9d) Translate and rotate the external mesh outer boundary to match the Lagrangian motion. Remesh the external mesh to optimize mesh quality.

In this way, the soft material may flow around the penetrator, moving through the ALE mesh, while the geometric details of the part corresponding to the harder material are preserved. A wide range of physics may be modeled in this fashion including penetration mechanics and metal turning.

Example calculations

In order to provide some validation of the SHISM algorithm and implementation, we review comparisons between experimentally measured and predicted results for penetration of a soft material (target) by a harder penetrator. Predicted maximum depth-of-penetration (*DOP*) is presented for normal and oblique impacts over a range of striking velocities. Here normal and oblique indicate that the velocity vector of the

penetrator center of mass is either aligned with the target normal (Angle-of-obliquity, AOO=0) or at an angle (AOO non-zero), respectively, Unless otherwise noted, the angle between the penetrator axis and the center-of-mass velocity vector (Angle-Of-Attack, *AOA)* is zero. The experimentally measured results used for comparison are taken from Piekutowski et al. (1999) and Warren and Poormon (2001). Details concerning the simulations (e.g. material models, penetrator geometry and impact conditions) are available in Bishop et al. (2005).

Figure 1 presents predicted and experimentally measured *DOP* for normal impact of a VAR 4340, 3 caliber-radius-head (CRH) steel penetrator with a 6061-T6511 aluminum target. The figure presents the experimentally measured results of Piekutowski et al. along with predicted results for three successively finer meshes (Ogive-1, Ogive-2 and Ogive-3 meshes respectively). It is clear from the figure that the predicted *DOP* results agree well with the experimental results up to striking velocities, V_s, of approximately 1.0 km/s for all three meshes. At V_s between 1.0 and 1.5 km/s, the Ogive-1 results are significantly lower than the measured values. However, the *DOP* results from the Ogive-2 mesh agreed very well with the experimental results in the 1.0 - 1.5 km/s velocity regime.

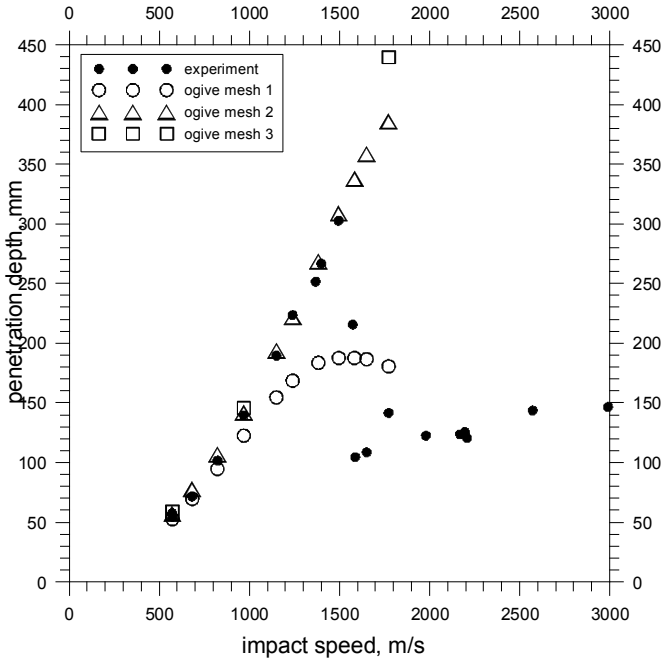

Figure 1. Comparison of predicted (Bishop et al., 2005) and experimentally measured (Piekutowski et al., 1999) DOP for a range of striking velocities. Results are plotted as a function of impact velocity for various levels of mesh refinement.

Note that for V_s > 1.5 km/s, the calculated maximum depth of penetration for the Ogive-2 and Ogive-3 meshes continues to increase with increased striking velocity. In contrast, while the experimentally measured values increase in the lower velocity range, they drop precipitously at 1.59 km/s. To explain this discrepancy, it is hypothesized that the *DOP* results are very sensitive to *AOA* for striking velocities ≥ 1.5 km/s. The experimental results of Warren and Poormon (2001) seem to confirm this when noting the large difference in reported *DOP* for the two cases at V_s = 1590 m/s (cf. Figure 1). These cases

were identical (within the reported uncertainty) with the exception of a 4° difference in *AOA* and a difference in *DOP* of approximately 100 mm. Although not shown explicitly in Figure 1, second-order spatial convergence of predicted *DOP* is observed (cf. Bishop et al., 2005).

Though the good comparison evident for sub-ordinate to ordinate velocities in Figure 1 is encouraging, penetration events can rarely be characterized by such idealized conditions (Goldsmith, 1999). Figure 2 illustrates a comparison of predicted and experimentally measured *DOP* for more realistic, oblique impacts. Specifically, results are presented for impacts associated with a range of striking velocities and *AOO* = 15°. The predicted results were obtained using the Ogive-2 mesh as this mesh provided converged results for the normal impact simulations (cf. Figure 1). The predicted results compared well to the experimental results of Piekutowski et al. (1999) as shown in the figure. Figure 3 shows the predicted rest position of the penetrator in the target and illustrates the turning induced by the non-normal impact.

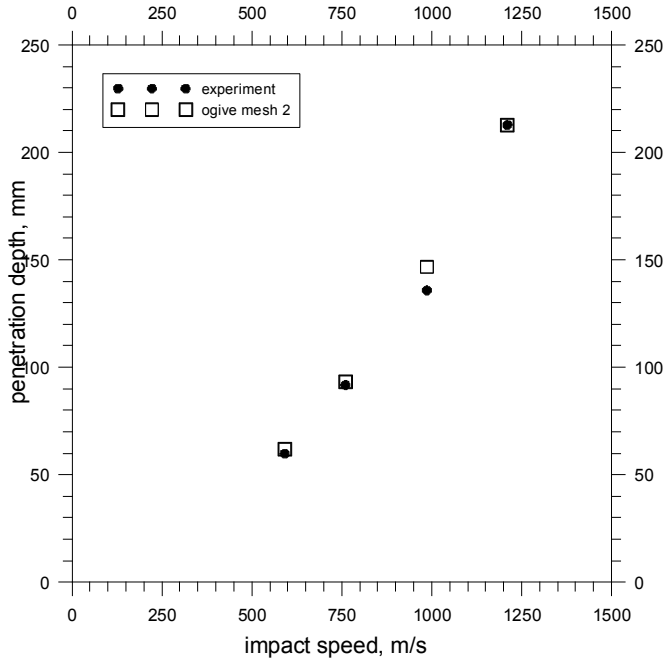

Figure 2. Comparison of predicted (Bishop et al., 2005) and experimental (Warren and Poormon, 2001) 15° oblique impact DOP as a function of striking velocity for the ogive-nose penetrator using an Ogive-2 mesh.

Predictions for *AOO* = 30° and 45° using the Ogive-2 mesh were attempted; however the resulting large penetrator distortion generally resulted in severe distortion of the ALE mesh in the target-region and subsequent failure of the remesh/remap algorithms. An example of the deformed mesh is shown in Figure 4 for AOO = 45° and V_s = 553 m/s. It is clear from the figure that the remesh algorithm is not able to prevent significant distortion of the target mesh. Indeed, experience with this type of simulation indicates that the equipotential smoothers available in ALEGRA tend to distort the mesh in unacceptable ways.

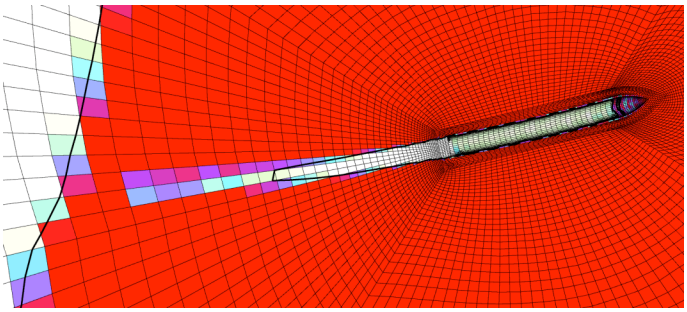

Figure 3. Final deformed mesh (Ogive-2) following a 15° oblique impact at a striking velocity of V_s = 1209 m/s (Bishop et al., 2005).

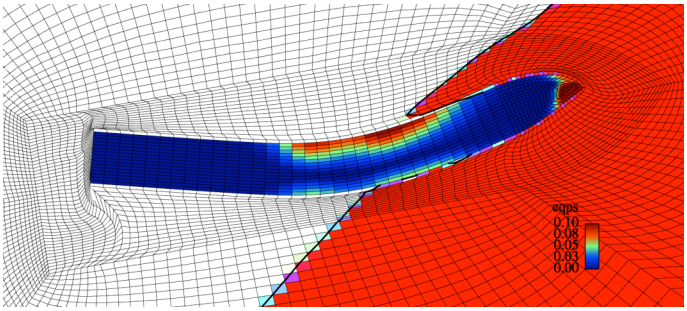

Figure 4. Final deformed mesh (Ogive-2) following a 45° oblique impact at a striking velocity of V_s = 553 m/s. Here, the legend indicates penetrator equivalent plastic strain (Bishop et al., 2005).

Directions for Better Remeshing

The discussion above suggests that advancements in remesh technology and their incorporation in ALEGRA may increase the applicable range of the SHISM algorithm. Although not discussed in detail above, the reader may have noted the partition of the target grid between a deforming ALE region near the penetrator and an Eulerian surrounding region. This mesh design is necessitated by the equipotential remesh algorithms currently implemented in ALEGRA. The scheme has been suggested by other ALE workers (Benson, 1989) and serves to constrain the region within which the remesh algorithm attempts to equalize ALE region element volumes. Were the entire region to be smoothed the resultant mesh would lose resolution near the penetrator while increasing far-field resolution. Unfortunately, for this problem, grid-refinement is needed primarily near the penetrator (region of high gradients in the field-variables). Although remesh weights may be used in conjunction with the equipotential smoother in an attempt to enforce refinement near the penetrator, significant skill is necessary to preserve a "good" mesh. Never-the-less equipotential smoothers only seek to equilibrate element volumes (perhaps weighted) and generally cannot sense and correct element distortion without significant user intervention.

These results suggest that mesh smoothing tools that preserve (to the extent possible) the good features of the user's original mesh are desirable. Recent developments in optimization-based remesh methodologies have resulted in just such methods (e.g.,

Knupp et al., 2002). These methods rely on some reference that describes a good mesh (e.g. the element Jacobians of the initial mesh) and the current mesh is moved to match those good qualities. These methods are currently being implemented in ALEGRA via the MESQUITE mesh smoothing package and results for representative calculations are encouraging.

ALEGRA/EP

On another research front a general methodology is being developed which does not rely on a viable contact algorithm but relies instead on mesh extension and overlap ideas.

The method is similar to the "ghost-fluid-method" from the Eulerian hydrodynamics community (Fedkiw, 1999). In this technology state information from one mesh is transferred to the other mesh in such a way as to be consistent with the jump condition holding at a slip contact discontinuity, i.e. continuous stress and normal velocity. Surface normals and material type are determined via a level set technology. No cell level multiple material technology as in a volume of fluid method is required at the expense of loss of exact conservation at material interfaces.

These ghost fluid ideas have more recently been extended to include Eulerian-Lagrangian coupling (Fedkiw, 2002; Arienti et al., 2003). In this method the Lagrangian region obtains Lagrangian boundary surface stress information via interpolation from the Eulerian region. The Eulerian ghost fluid cells are filled in alternative ways using normal velocity information from the Lagrangian mesh.

Our approach for Lagrangian - ALE coupling is slightly different and has been influenced by the Lagrangian – Eulerian coupling methodology developed at Sandia called ZAPOTEC which is a coupling methodology between PRONTO and CTH (Bessette, 2002).

Instead of coupling two distinct codes we are attempting to more closely integrate the Lagrangian step computations in both the Lagrangian mesh and the ALE mesh. We require that a layer of ghost cells be generated at the Lagrangian interface surface. Thus in this sense we have a fully overlapped mesh similar to the ghost fluid method.

In this approach, two separate computations are synchronized in time. Each problem is run on an independent mesh. For our purposes, a relatively harder body with initial velocity conditions is described with a body-fitted Lagrangian mesh. The target environment is described by a structured multiblock ALE mesh. Data is transferred between the meshes to facilitate the solution.

For the target material, data from the penetrator is transferred from the unstructured mesh to the structured mesh. However, because the unstructured mesh is body-fitted to the penetrator, a layer of elements is constructed surrounding the outer surface of the penetrator. We call this set of elements, phantom elements. Data transferred from the target material in the structured mesh is placed in the phantom elements. Phantom elements are not actually created as full element objects but the information is stored in the surface elements

The solution proceeds following the general steps described for ALEGRA, through step 5. At this point, the meshes are coupled through a transfer of data and a subsequent momentum balance. Among other quantities, an element-centered velocity and the

element density produce a density based momentum. The density and momentum are transferred from the structured mesh (target) to the phantom elements of the unstructured mesh and from the unstructured mesh (penetrator) to the structured mesh. The transfer is accomplished as a volume weighted overlap mapping using the ACME library (Brown, et al., 2003).

After the transfer, the density and momentum from the structured mesh are assembled to the nodes of the phantom mesh. Similarly, mass and momentum of the penetrator material adjacent to the phantom mesh are assembled to the nodes on the surface. The momentum is balanced across the interface between the penetrator and phantom elements, producing a velocity that accounts for the interaction between the penetrator and the target materials. The momentum balance solves a contact problem between two bodies.

Similar to the solution on the unstructured mesh, the density and momentum of the penetrator, transferred into the structured mesh, are assembled to the nodes of the structured elements along with the density and momentum of the existing target material. The momentum balance between the transferred penetrator material and the target material produces a velocity for the node accounting for the interaction of the materials.

This corrected velocity at the interface between penetrator and target on both meshes allows the completion of the equations of motion. The solution on both meshes then resumes with Step 7, the calculation of the gradient of the velocity field and, subsequently, the strain rate.

Generally, the remesh and remap only occurs on the structured mesh. The portion of the structured mesh involved in the overlap calculation is Eulerian. Other portions of the structured mesh may be ALE or Lagrangian, depending on the expected movement of the target material. The unstructured mesh describing the penetrator is treated as Lagrangian. However, this is not a strict requirement of the method.

The ALEGRA/EP algorithm is still in development and significant software infrastructure is in place. Relative to the ALEGRA/SHISM method, the algorithm allows for simpler problem set up, more complicated structured meshes and does not inherently rely on the remesh to maintain the mesh surrounding the penetrator. However, the development of a consistent and reliable interface coupling algorithm between the Lagrangian penetrator and the target material in the structured mesh is still in progress.

Example calculations

Because the ALEGRA/EP algorithm is still in development, it has not yet been subjected to validation calculations such as those described above for ALEGRA/SHISM. Some test calculations have been carried out to examine the ability of the algorithm to support typical calculations of interest on parallel architectures.

Shown below is a test calculation of a penetrating body obliquely impacting a homogeneous target block. The Lagrangian penetrator mesh and the target mesh are overlaid, showing the interaction of the two materials as the penetration has progressed. The target region consists of an Eulerian mesh in the overlap area, surrounded by Lagrangian mesh. In this case, the target material has started to displace the top surface of the Lagrangian mesh and produced a kink between the Eulerian and Lagrangian mesh which effectively ended the calculation.

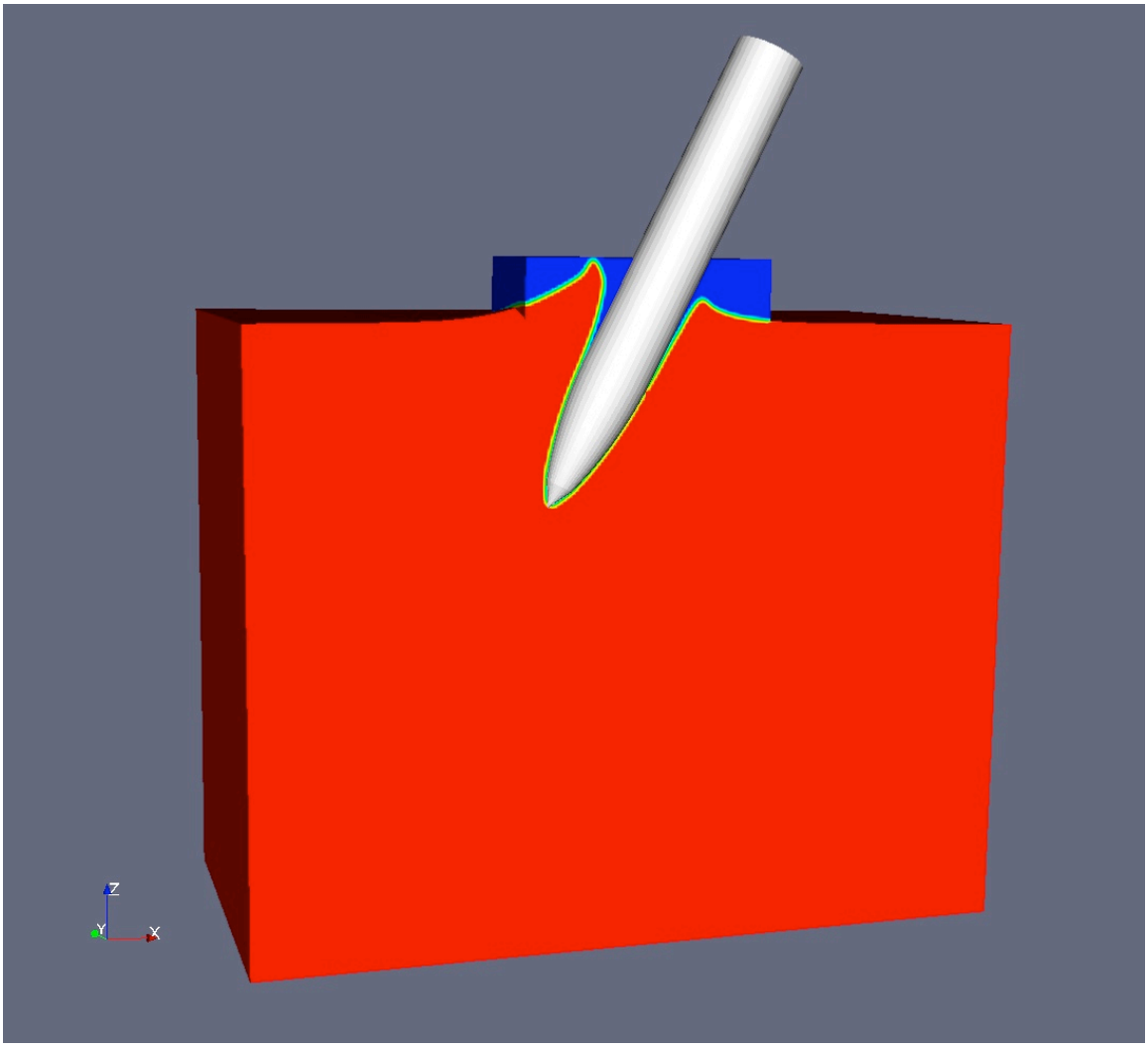

Figure 5. Test calculation for a Lagrangian penetrator interacting with an Eulerian region inside a target Lagrangian mesh using the ALEGRA/EP algorithm.

Conclusions

Two distinct algorithms for coupling Lagrangian and ALE solution domains have been implemented within ALEGERA. The ALEGRA/SHISM algorithm is based on coupling a Lagrangian and a multi-material ALE mesh through a Lagrangian interface using standard explicit transient dynamics contact algorithms . This algorithm is at a fairly advanced development state, and its results compare favorably to experiments. The ALEGRA/EP algorithm uses an overlapping grid approach that offers the advantages of simplicity and robustness. This algorithm is too immature for quantitative comparison to experiments, but progress towards this end shows promise.

Acknowledgements

Many developers and analysts have made important contributions to the improvement of the ALEGRA/NEVADA code base. In particular we mention that the original SHISM concept was developed by K. G. Budge and J. S. Peery. K. H. Brown was key in the

continued development of the SHISM capability as well as the current ALEGRA/EP algorithm. H. Meyer made primary contributions to the phantom mesh generation algorithms. L. N. Kmetyk has performed a number of verification and validation calculations with both SHISM and EP.

Sandia is a multiprogram laboratory operated by Sandia Corporation, a Lockheed Martin Company, for the United States Department of Energy's National Nuclear Security Administration under contract DE-AC04-94AL85000.

References

Arienti, M., Hung, P., Morano, E. and Shepard, J. E., "A level set approach to Eulerian-Lagrangian coupling," *J. Computational Physics,* **185**, 213-251 (2003).

Benson, D., "An efficient, accurate, simple ALE method for nonlinear finite element programs," *Computer Methods in Applied Mechanics and Engineering*, **72**, 302-350 (1989).

Bessette, G., Vaughan, C., and Bell, R., "*Zapotec: a coupled Euler-Lagrange program for modeling earth penetration*," Proceedings of the 73rd Shock and Vibration Symposium, Newport, RI, November 18-22, (2002).

Bishop, J. E., Voth, T. E., and Brown, K. H., "Semi-Infinite Target Penetration by Ogive-Nose Penetrators: ALEGRA/SHISM Code Predictions for Ideal and Non-Ideal Impacts," Proceedings of the ASME PVP2005, Denver, CO, July 17-21 (2005).

Brown, K., Glass, M., Gullerud, A., Heinstein, M., Jones, R. and Voth, T., "ACME: Algorithms for Contact in a Multi-Physics Environment," SAND2003-1470, Sandia National Laboratories, Albuquerque, NM (2003).

Carroll, S. K., Drake, R. R., Hensinger, D. M., Luchini, C. B., Petney, S. V., Robbins, J., Robinson, A. C., Summers, R. M., Voth, T. E., Wong, M. K., Brunner, T. A., Garasi, C. J., Haill, T. A. and Mehlhorn, T. A., *ALEGRA: Version 4.6*, Sandia National Laboratories, Albuquerque, NM, SAND2004-6541 (2005).

Fedkiw, R. P., Aslam, T., Merriman, B. and Osher, S., "A Non-oscillatory Eulerian Approach to Interfaces in Multimaterial Flows (the Ghost Fluid Method)," *J. Computational Physics,* **52**, 457-492 (1999).

Fedkiw, R. P., "Coupling an Eulerian Fluid Calculation to a Lagrangian Solid Calculation with the Ghost Fluid Method," *Journal of Computational Physics,* **175**, 200-224 (2002).

Goldsmith, W., "Non-ideal projectile impact on targets," *International Journal of Impact Engineering*, 1999, **22**, 95-395 (1999).

Knupp, P., Margolin, L., and Shashkov, M., "Reference Jacobian optimization-based rezone strategies for Arbitrary Lagrangian Eulerian methods," *Journal of Computational Physics*, **176**, 93-128 (2002).

Peery, J. and Carroll, D., "Multi-material ALE methods in unstructured grids," *Computer Methods in Applied Mechanics and Engineering*, **187,** 591-619 (2000).

Piekutowski, A., Forrestal, M., Poormon, K., and Warren, T., "Penetration of 6061-T6511 aluminum targets by ogive-nose steel projectiles with striking velocities

between 0.5 and 3.0 km/s," *International Journal of Impact Engineering*, **23**, 723-734 (1999).

Taylor, L. and Flanagan, D., *PRONTO3D: A three-dimensional transient solid dynamics program*, Sandia National Laboratories, Albuquerque, NM SAND87-1912 (1987).

Warren, T. and Poormon, K., "Penetration of 6061-T6511 aluminum targets by ogive-nosed VAR 4340 steel projectiles at oblique angles: experiments and simulations," International *Journal of Impact Engineering*, **25**, 993-1022 (2001).